Proc. NIPR Symp. Antarct. Meteorites, **9**, 20–36, 1996

YAMATO-86789: A HEATED CM-LIKE CARBONACEOUS CHONDRITE

Kenji MATSUOKA, Tomoki NAKAMURA, Yoshihiro NAKAMUTA and Nobuo TAKAOKA

Department of Earth and Planetary Sciences, Faculty of Science, Kyushu University, Hakozaki 33, Fukuoka, 812–81

Abstract: We have studied the mineralogy and petrology of the Yamato(Y)-86789 meteorite and concluded that this meteorite is a new member of heated carbonaceous chondrites with CI-CM affinities. Y-86789 contains 14 vol% of translucent chondrules which mainly consist of fibrous phyllosilicate-like materials. The high abundance of the phyllosilicate-like minerals in chondrules suggests severe aqueous alteration. Major parts of the matrix are also composed of the phyllosilicate-like materials. The phyllosilicate-like materials have compositions of a mixture of serpentine and saponite. However, the phyllosilicate-like materials show consistently high analytical totals; thus, they are dehydrated. X-ray diffraction measurements of the phyllosilicate-like materials reveal that they are mainly composed of olivine. Diffractions from serpentine and saponite are absent from the X-ray powder patterns. These results suggest that Y-86789 has experienced heating and the phyllosilicate minerals which were once present in Y-86789 were dehydrated to form anhydrous materials such as olivine.

Y-86789 has textural, mineralogical, and compositional characteristics similar to those of Y-86720, which is one of the three unusual Antarctic carbonaceous chondrites with CI-CM affinities that show evidence of dehydration. Chondrules are completely replaced by the phyllosilicate-like materials and are surrounded by fine-grained rims. Some chondrules contain Ca-carbonates. There is an abundance of troilite in the matrix, but magnetite and PCP, which are common in CM chondrites, are absent. Some large troilite grains have a euhedral lath-like morphology. The bulk chemical composition of Y-86789 is also similar to that of Y-86720. On the basis of these similarities, we propose that Y-86789 and Y-86720 are paired meteorites.

1. Introduction

CI and CM carbonaceous chondrites are primitive meteorites, but are known to be affected by secondary aqueous alteration (*e.g.*, DUFRESNE and ANDERS, 1962; RICHARDSON, 1978; MCSWEEN, 1979, 1987; BUNCH and CHANG, 1980; TOMEOKA and BUSECK, 1985; FREDRIKSSON and KERRIDGE, 1988; TOMEOKA, 1990a). Recently, several unusual carbonaceous chondrites with CI-CM affinities that experienced thermal metamorphism after aqueous alteration have been found among the Antarctic meteorites. They are important samples experienced more advanced evolution processes than usual CI-CM carbonaceous chondrites. Three Antarctic meteorites, Belgica(B)-7904, Yamato(Y)-82162, and Y-86720, have already been reported as such meteorites, which had been studied by a research consortium (Leader: Y. IKEDA) (*e.g.*, AKAI, 1990; TOMEOKA *et al.*, 1989a, b; TOMEOKA, 1990b; IKEDA, 1991; KIMURA and IKEDA, 1992; IKEDA *et al.*, 1992). The results are summarized by IKEDA (1992).

All these unusual carbonaceous chondrites show whole-rock oxygen isotope ratios similar to those of CI chondrites (MAYEDA and CLAYTON, 1990), while elemental abundances (*e.g.*, Zn/Mn *vs.* Al/Mn) vary one another; B-7904, Y-82162, and Y-86720 have elemental abundances of CM, CI, and intermediate between CI-CM, respectively (KALLEMEYN, 1988). Further, mineralogical features are also variable among them. B-7904 and Y-86720 are petrologically similar to CM chondrites, and Y-82162 is similar to CI chondrites (*e.g.*, IKEDA, 1992). The most distinguishable characteristics of these meteorites from normal CI-CM chondrites are; (1) microprobe analyses of phyllosilicates in these meteorites show higher analytical totals than ordinary phyllosilicates, suggesting low H_2O contents (BISCHOFF and METZLER, 1991), (2) wet chemical analyses of these meteorites show low H_2O contents (HARAMURA *et al.*, 1983; TOMEOKA *et al.*, 1989a, b), and (3) transmission-electron microscope (TEM) observations reveal that the phyllosilicates in these meteorites are decomposed to nearly amorphous materials and fine grains of olivine (AKAI, 1988, 1990, 1994; TOMEOKA *et al.*, 1989a, b). All these analyses suggest that these meteorites were dehydrated by metamorphic heating.

Y-86789 is an Antarctic carbonaceous chondrite that consists largely of dark and fine-grained materials. As a preliminary observation, YANAI and KOJIMA (1987) have classified this meteorite as a carbonaceous chondrite, but the mineralogical characteristics of this meteorite are yet to be studied. In this paper, we present our electron-microscope and X-ray studies of the Y-86789 meteorite. Our results indicate that Y-86789 experienced mild heating after aqueous alteration, and that this meteorite is a new member of heated carbonaceous chondrites with CI-CM affinities.

2. Sample and Analytical Methods

A polished thin section and a polished section were prepared from a meteorite chip of Y-86789. They were studied using an optical microscope and an electron-probe microanalyzer (EPMA: JEOL JCXA-733 Superprobe) equipped with wave-length-dispersive X-ray spectrometers (WDS). WDS analyses were obtained at 15 kV and 10 nA with a focused beam ~3 μm in diameter. A defocused beam 50 μm in diameter was also employed to determine bulk composition of the meteorite. The correction for quantitative chemical analysis was made by ZAF method.

After petrographic characterization, portions of the chondrules and matrix approximately 100×100×100 μm in size were extracted from the polished section under a binocular microscope using an edged tool. The extracted chondrule and matrix were mounted on thin glass fibers with 10 μm in diameter and were exposed to Cr Kα X-ray in a Gandolfi camera. The X-ray generator was operated at 35 kV and 20 mA. The X-ray photographs were scanned by a photo densitometer and were taken into a computer in order to read precise peak positions.

Modal analysis of chondrules was made by transferring shapes of the objects in a backscattered electron (BSE) image to a computer system, then numbers of pixels within the objects were counted by using the Flexi Trace software.

3. Results

3.1. General description

Y-86789 consists mainly of dark brownish to black, fine-grained matrix with chondrules embedded in the matrix. The modal abundance of the chondrules is approximately 14 vol% lying within the range of CM chondrites (McSween, 1979). Many chondrules are surrounded by fine-grained rims similar to the accretionary dust mantles found in CM chondrites (METZLER and BISCHOFF, 1987, 1989, 1990; METZLER *et al.*, 1988, 1992) (Figs. 1a and b). These observations indicate that Y-86789 has an overall texture similar to that of CM chondrites. However, poorly characterized phases (PCP) and magnetite that are common in CM chondrites are absent from Y-86789. Instead, large amounts of troilite and minor kamacite and taenite occur in the matrix. A bulk chemical composition of the meteorite was determined by averaging 166 defocused beam analyses and is shown in Table 1.

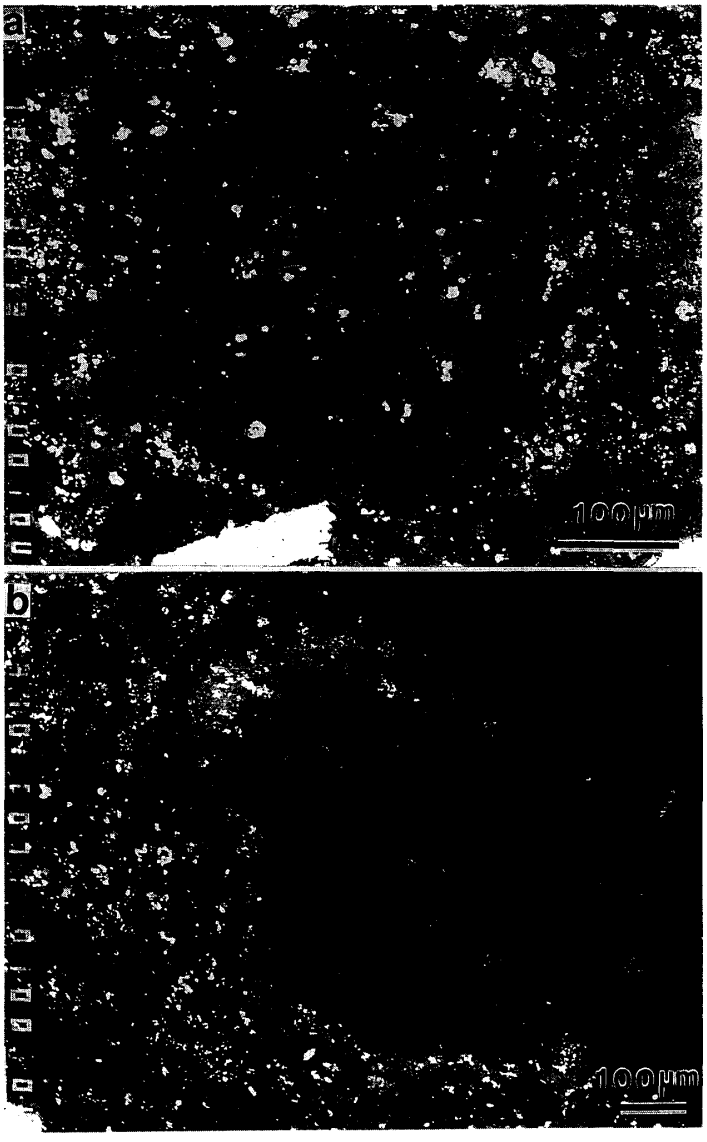

Fig. 1. BSE images of chondrules.
(a) A chondrule with fibrous texture is shown. Troilite grains are surrounded by bright halos.
(b) A chondrule with fibrous and massive texture is shown. Many ovoidal inclusions are contained in this chondrule. Troilite grains are concentrated between the chondrule and the rim.

Table 1. Major element chemical composition of Y-86789 with the reference of those of B-7904, Y-82162, and Y-86720 (wt%).

	Y-86789*	B-7904#	Y-82162#	Y-86720#
SiO_2	29.34	31.49	26.99	30.69
TiO_2	0.08	0.16	0.23	0.09
Al_2O_3	1.96	3.30	2.26	3.83
FeO	19.09	21.91	12.94	19.77
MnO	0.27	0.25	0.31	0.18
MgO	21.06	23.71	20.91	22.72
CaO	2.26	2.22	2.04	2.02
Na_2O	0.37	0.66	0.87	0.66
K_2O	n.d.	0.04	0.13	0.04
Cr_2O_3	0.42	0.50	0.48	0.45
NiO	0.90	1.21	1.28	1.16
FeS	6.60	11.45	20.08	13.22
Total	82.35	96.90	87.80	94.83

n.d.: not detected

The composition of Y-86789 was measured by averaging 166 deforcused-electron beam analyses with an EPMA. The compositions of the other three meteorites are results of wet chemical analyses. Analyst: H. HARAMURA. Data; HARAMURA *et al.* (1983), TOMEOKA *et al.* (1989a, b).

* All SO_3 contents in this bulk analysis were recalculated as FeS.

$H_2O(+)$, $H_2O(-)$, P_2O_5, and Co are not shown here, because these oxides and metal were not measured in our EPMA analyses. Fe and Fe_2O_3 are recalculated and included in FeO.

3.2. *Chondrules*

Chondrules in Y-86789 show subrounded or irregular outlines and typically range from 600 to 750 μm in diameter, while some chondrules and their fragments are smaller than a few hundreds of microns. All chondrules are composed mainly of dark brownish, translucent materials with variable amounts of opaque minerals. The translucent materials show fine-grained and fibrous texture which is reminiscent of phyllosilicate (Fig. 2a); thus we hereafter call these translucent materials phyllosilicate-like materials. Anhydrous silicate minerals such as olivine and pyroxene of optically visible sizes are absent. These observations suggest that extensive aqueous alteration occurred and replaced anhydrous silicate minerals in the chondrules with phyllosilicate minerals.

Electron-microscope observations show that most chondrules are composed of fibrous or massive phyllosilicate-like materials (Figs. 1a and b). The phyllosilicate-like materials often contain ovoidal inclusions 10–60 μm in diameter, and vainlets 20–150 μm in length and 2 to 30 μm in width (Fig. 2b). The phyllosilicate-like materials in both fibrous and massive forms are rich in SiO_2 (42–48 wt%), MgO (25–32 wt%), and FeO (12–19 wt %) and contain minor amounts of Al_2O_3 (2–6 wt%) (Table 2). Their chemical compositions are fairly homogeneous and lie between serpentine and saponite solid solution lines in the (Si+Al)-Mg-Fe ternary diagram (Fig. 3), suggesting a mixture of serpentine- and saponite-type phyllosilicates. However, the phyllosilicate-like materials have high analytical totals (>94 wt%) compared with normal phyllosilicate (Table 2), indicating

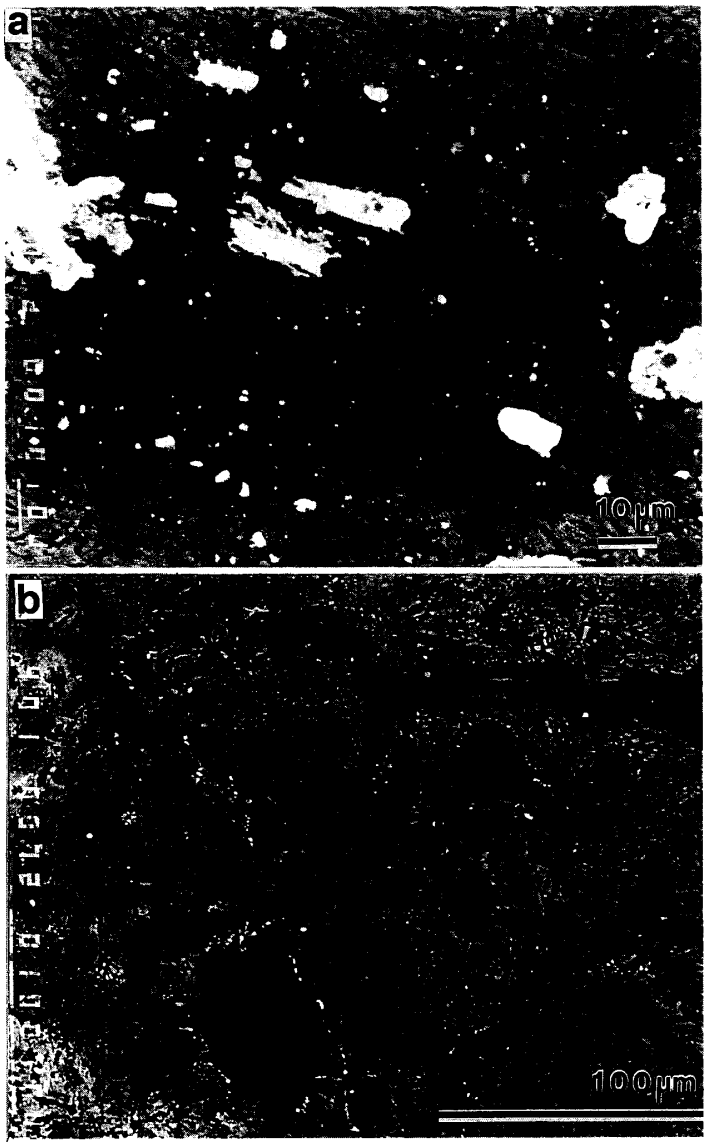

Fig. 2. BSE images of (a) fibrous texture reminiscent of phyllosilicate and (b) massive and fibrous texture containing ovoidal inclusions of the phyllosilicate-like materials in chondrules.

that they are dehydrated. Further, many vacant spaces are found between the phyllosilicate-like materials in BSE images (Fig. 2a), suggesting contraction during heating and dehydration. X-ray diffraction measurements reveal that the phyllosilicate-like materials in the chondrules mainly consist of olivine (Fig. 4a). No reflection of serpentine, saponite, or other phyllosilicate minerals is recognized. The phyllosilicate-like materials are thus likely to be produced by a thermal decomposition process of phyllosilicate to form olivine. Since serpentine and saponite have higher SiO_2 contents than olivine, the phyllosilicate-like materials should contain amorphous silica phases which do not appear in the X-ray powder pattern.

Some chondrules contain Al-rich portions (7–19 wt% in Al_2O_3) which are unusually enclosed in the massive phyllosilicate-like materials. In the Al-rich portions, Al is often concentrated in phases that have euhedral parallelogram morphology (Figs. 5a and b). These phases may correspond to "High-Al phases (HA-phases)" in Y-86720 reported by

Table 2. Representative chemical compositions of phyllosilicate-like materials and associated phases in Y-86789 (wt%).

	Phyllosilicate-like materials (chondrules)			HA-Phases			Fe-rich halos in chondrules		
SiO_2	44.01	46.42	47.64	41.51	40.29	34.19	35.84	26.02	36.89
TiO_2	0.08	0.10	0.14	0.14	0.07	0.07	0.07	0.10	0.14
Al_2O_3	2.24	5.35	2.47	10.93	12.98	18.53	2.35	1.11	6.77
Cr_2O_3	0.35	1.98	0.50	0.04	2.03	0.35	0.49	0.63	2.22
FeO	14.83	16.66	12.75	13.66	15.61	19.91	33.78	49.38	25.04
MnO	0.14	0.05	0.08	0.03	0.04	0.09	0.45	0.27	0.12
MgO	32.62	29.23	32.40	27.37	29.03	23.06	26.05	17.97	21.25
CaO	0.25	0.18	0.15	0.12	0.01	0.29	0.17	0.37	0.17
Na_2O	0.31	0.63	0.44	0.64	0.94	1.33	0.36	0.14	0.64
K_2O	n.d.	n.d.	n.d.	n.d.	n.d.	n.d.	n.d.	n.d.	n.d.
Total	94.83	100.60	96.57	94.44	101.00	97.82	99.56	96.00	93.24

	Ovoidal inclusion			Phyllosilicate-like materials (matrix)			Fe-rich halos in matrix		
SiO_2	42.00	42.60	46.86	46.45	44.78	46.49	36.36	31.80	29.20
TiO_2	0.05	0.11	0.13	0.01	0.11	0.07	0.05	0.03	0.04
Al_2O_3	3.50	3.21	2.89	0.09	2.92	3.50	2.31	2.34	2.01
Cr_2O_3	6.82	2.14	2.76	0.20	0.60	0.70	0.39	0.42	0.45
FeO	16.70	22.30	19.57	14.91	18.97	20.37	34.18	44.78	47.62
MnO	0.27	0.20	0.08	0.32	0.34	0.14	0.14	0.19	0.44
MgO	29.94	25.59	28.51	30.71	25.04	25.92	24.00	19.89	19.62
CaO	0.10	0.61	0.67	0.35	1.58	0.91	0.30	0.47	1.08
Na_2O	0.67	0.71	0.30	0.06	0.58	0.63	0.35	0.41	0.24
K_2O	n.d.	n.d.	n.d.	n.d.	n.d.	n.d.	n.d.	n.d.	n.d.
Total	100.05	97.47	101.77	93.10	94.92	98.73	98.08	100.33	100.70

n.d.: not detected.

Tomeoka *et al.* (1989b). Their chemical compositions are shown in Table 2 and plotted in Fig. 3. Chondrules containing Ca-rich phases also occur (Table 3 and Fig. 6). Figure 7 indicates that these Ca-rich phases are mixtures of the phyllosilicate-like materials and minor amounts of Ca-carbonates, although Ca-carbonates are too small to resolve chemical compositions by an EPMA.

The opaque minerals in the chondrules are mainly troilite with minor ilmenite (TiO_2: 50.03%, FeO: 43.16%, MnO: 0.87%, MgO: 5.57% in molecular ratio). BSE images show that some troilite grains in the chondrules have bright halos several to a few tens microns wide (Fig. 1a), which are composed of materials containing large but variable amounts of FeO (20–50 wt%) with constant Mg/Si ratios (Table 2 and Fig. 3). Figure 3 shows that the compositions of the halos lie between the cluster of the normal phyllosilicate-like materials in the chondrules and the Fe apex, suggesting that these Fe-rich halos were produced by diffusion of Fe from enclosed troilite grains.

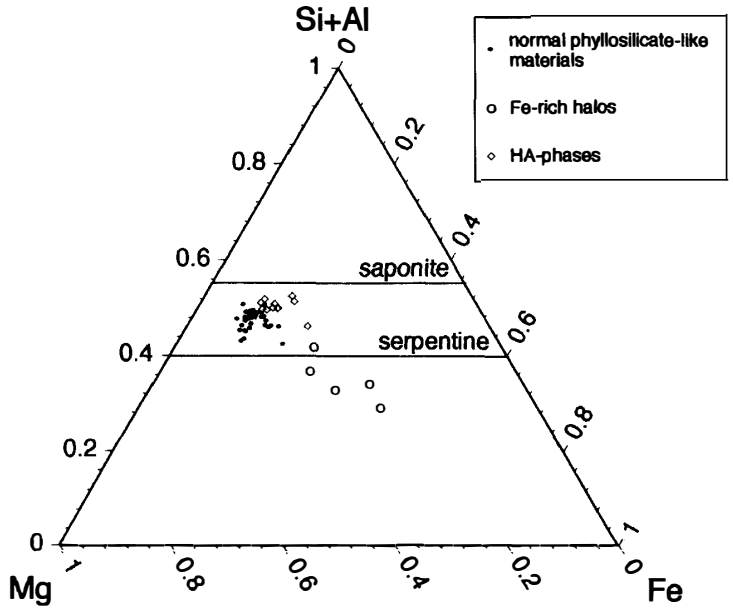

Fig. 3. A (Si+Al)-Fe-Mg ternary diagram in terms of atomic ratio of the phyllosilicate-like materials in the chondrules (solid circles). Open circles and open diamonds are Fe-rich halos surrounding troilite grains and the HA-phases, respectively.

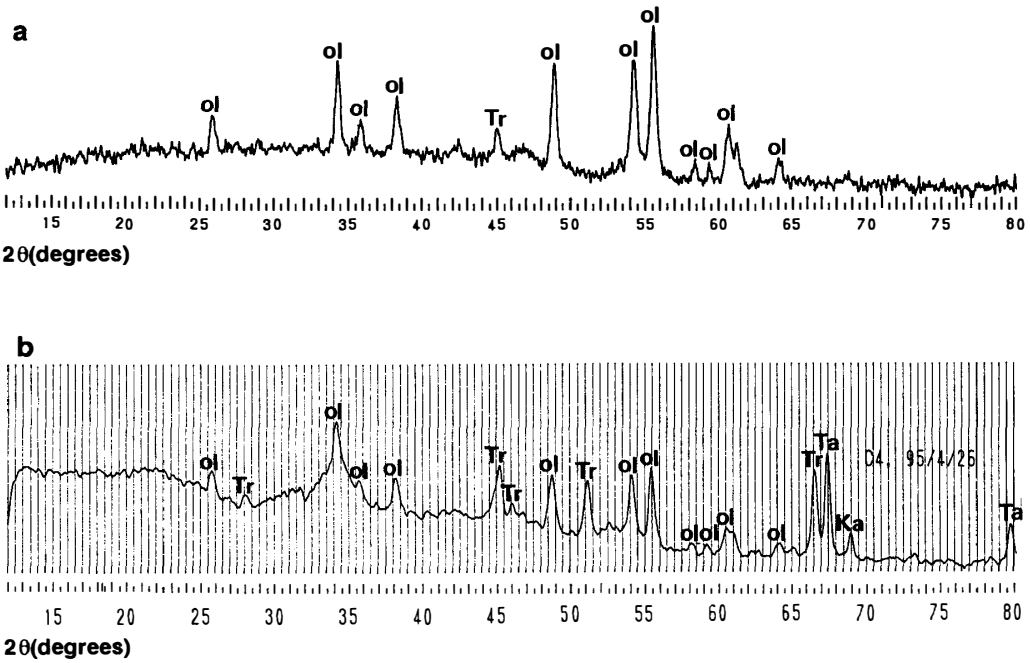

Fig. 4. X-ray powder patterns (Cr, Kα) of a chondrule (a) and matrix (b) in Y-86789. Tr, Ta, Ka, and ol indicate reflections from troilite, taenite, kamacite, and olivine, respectively. Reflections of silicate minerals in both (a) and (b) are only those of olivine. In (b), unusual broadening observed in basal reflections of olivine suggests existence of incompletely crystallized olivine.

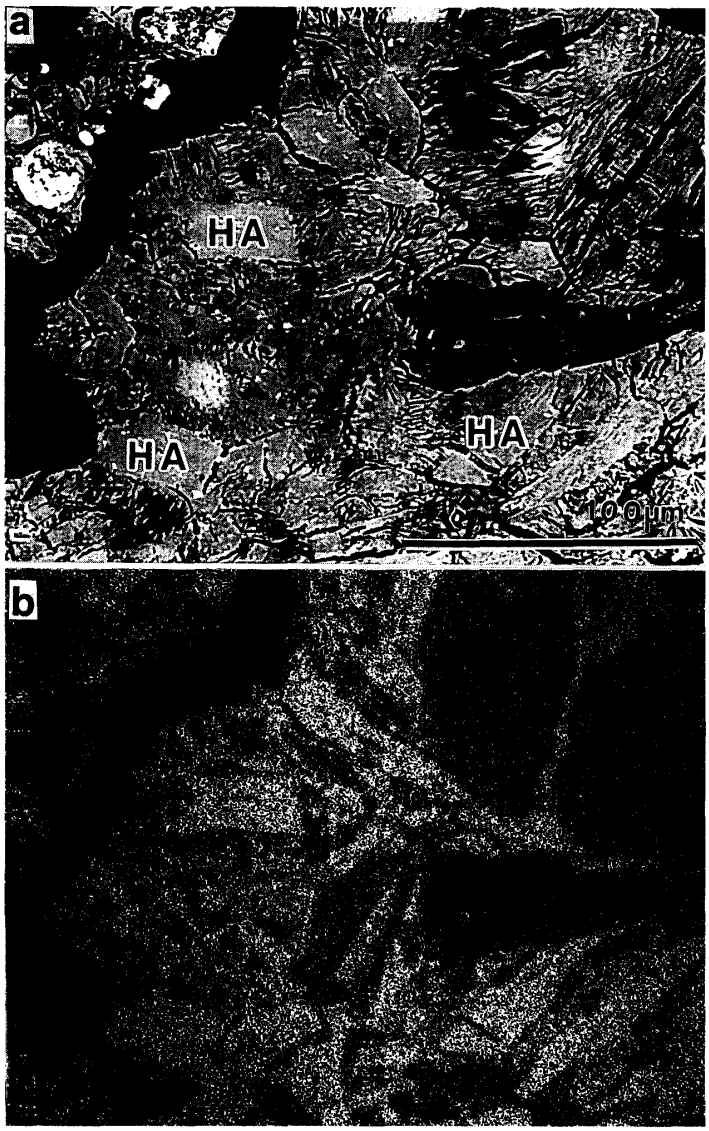

Fig. 5. (a) The HA-phases (HA, slightly bright part) in massive phyllosilicate-like materials in a chondrule. Some parts of the HA-phases have euhedral parallelogram morphology (BSE image).
(b) "Al" X-ray image of (a).

Table 3. Representative chemical compostions of Ca-rich phases in a chondrule (wt%).

SiO_2	36.27	32.54	36.81	36.66
TiO_2	0.16	0.12	0.15	0.19
Al_2O_3	3.31	4.63	4.25	5.17
Cr_2O_3	0.64	0.69	0.50	0.61
FeO	8.27	6.96	5.81	5.71
MnO	1.06	0.82	0.75	0.91
MgO	25.15	20.99	32.06	29.69
CaO	25.99	30.67	13.60	18.75
Na_2O	0.04	0.06	0.08	0.03
K_2O	n.d.	n.d.	n.d.	n.d.
Total	100.89	97.48	94.01	97.72

n.d.: not detected

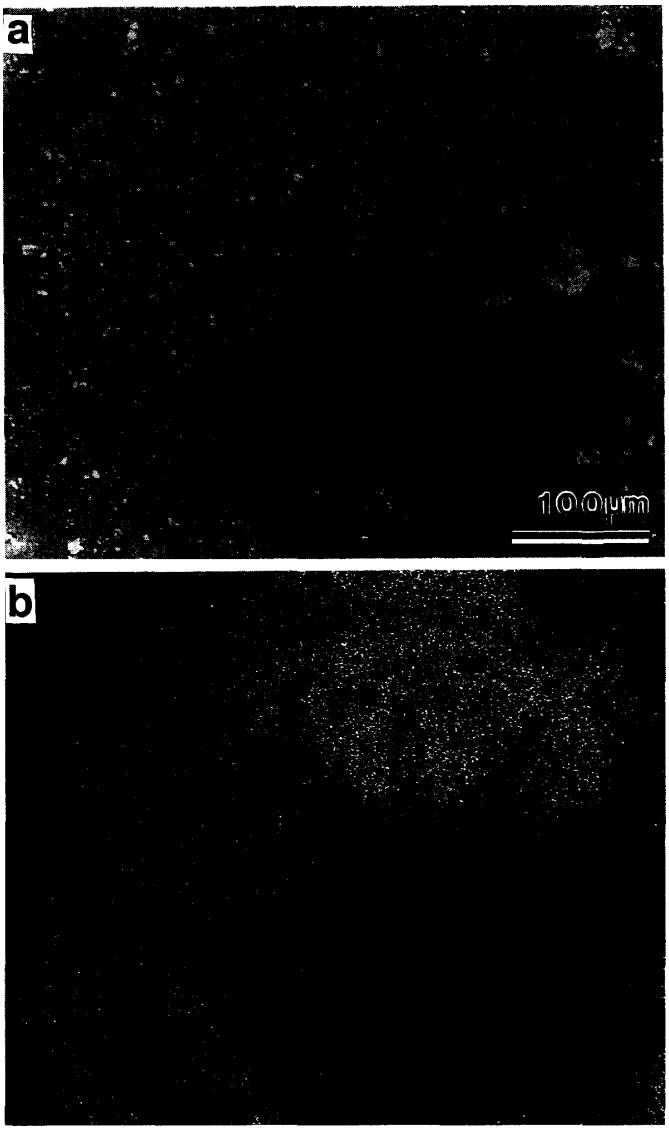

Fig. 6. (a) BSE image and (b) "Ca" X-ray image of an irregular-shaped, Ca-rich chondrule with fibrous texture.

3.3. Matrix

Matrix of Y-86789 also consists mainly of the fine-grained phyllosilicate-like materials similar to those in the chondrules, although the phyllosilicate-like materials in the matrix are very fine-grained and don't have fibrous or massive texture such as those in the chondrules. The phyllosilicate-like materials in the matrix show chemical compositions of a mixture of serpentine- and saponite-type phyllosilicate minerals (Table 2 and Fig. 8). However, X-ray measurements reveal that matrix consists of olivine, troilite, taenite, and kamacite (Fig. 4b). No reflection of phyllosilicate minerals is recognized. Thus, the phyllosilicate-like materials in the matrix are also likely to be dehydrated and decomposed to olivine and amorphus Si-rich phases as those in the chondrules. In some X-ray powder patterns, basal reflections of olivine show unusual broadening (Fig. 4b) due to low crystallinity of olivine. This might be a result of incomplete crystallization of olivine after decomposition of phyllosilicate minerals.

Of particular interest in the matrix is a high abundance of porous aggregates that

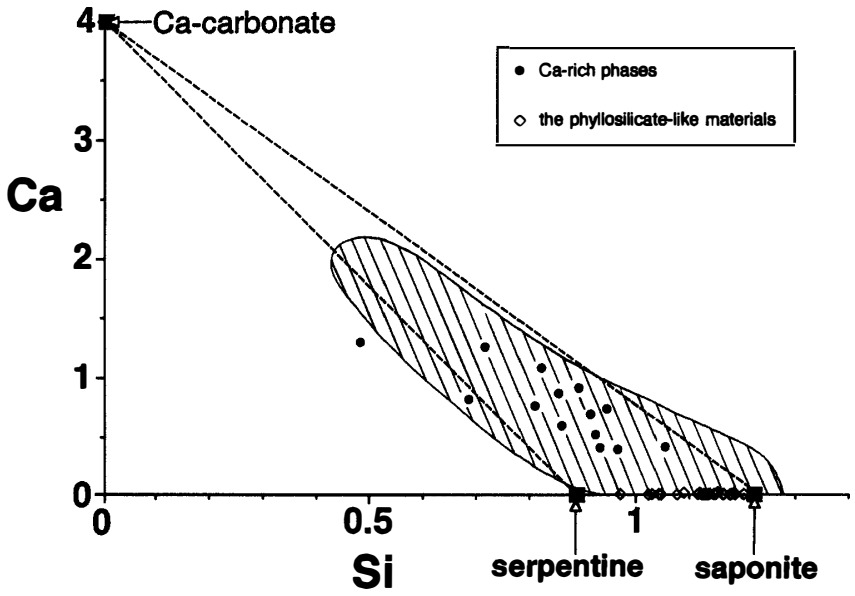

Fig. 7. Silicon and Ca atomic contents of Ca-rich phases in chondrules, normalized by O=4. Solid circles are Ca-rich phases and open diamonds are the phyllosilicate-like materials in the chondrules. Compositional range of Ca-rich phases in Y-86720 (IKEDA et al., 1992) is shown by a dashed area for comparison.

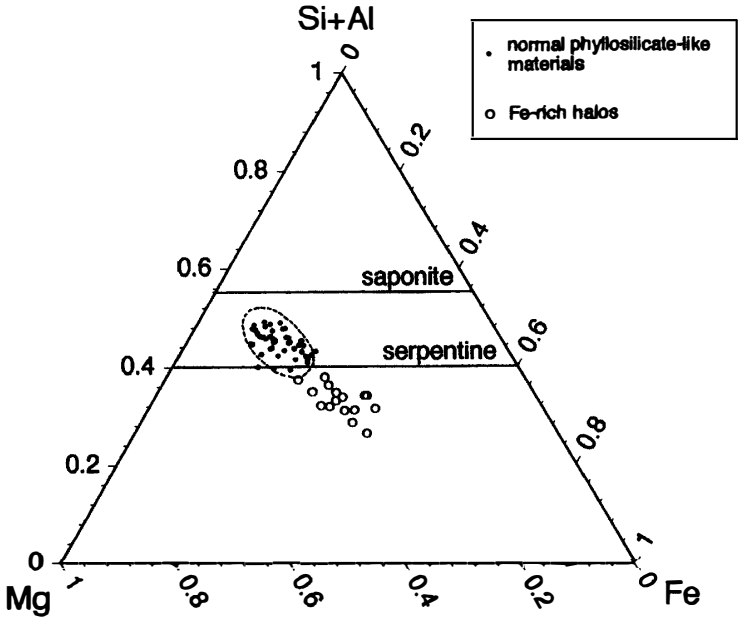

Fig. 8. A (Si+Al)-Fe-Mg ternary diagram in terms of atomic ratio showing compositions of the phyllosilicate-like materials (solid circles) in the matrix. Open circles are Fe-rich halos surrounding troilite grains. A compositions of the matrix of Y-86720 reported by TOMEOKA et al. (1989b) is shown for comparison by dashed line.

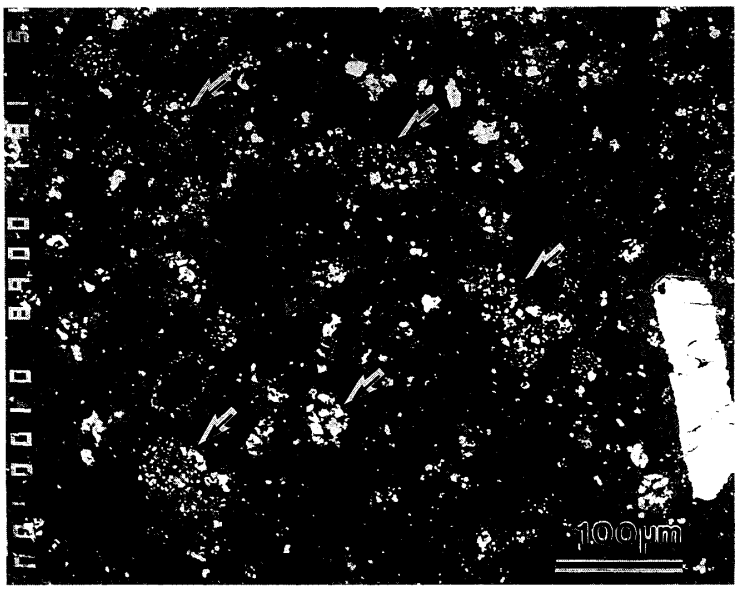

Fig. 9. A BSE image of the matrix. Many troilite grains are dispersed. Troilite grains are surrounded by bright Fe-rich halos. There are abundant porous aggregates (indicated by arrows), which include variable amounts of small grains that consist mainly of troilite.

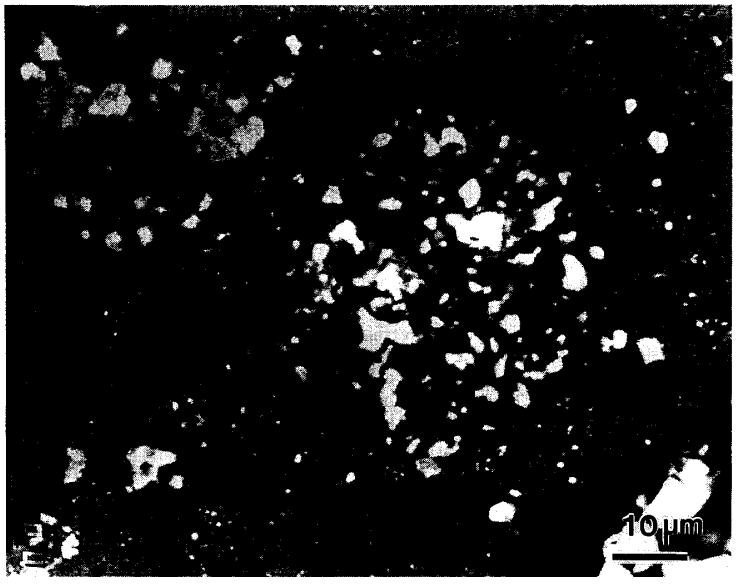

Fig. 10. A BSE image of a rounded porous aggregate in the matrix that contains small troilite grains.

Table 4. Representative chemical compositions of porous aggregates (wt%).

Cr_2O_3	0.11	0.20	0.22	0.18
FeO	22.13	24.96	17.62	58.72
MnO	0.37	0.18	0.34	0.24
CaO	3.50	0.47	15.13	0.15
SO_3	0.50	14.06	12.18	14.96
NiO	0.36	0.22	0.12	0.28
Total	26.97	40.09	45.61	74.53

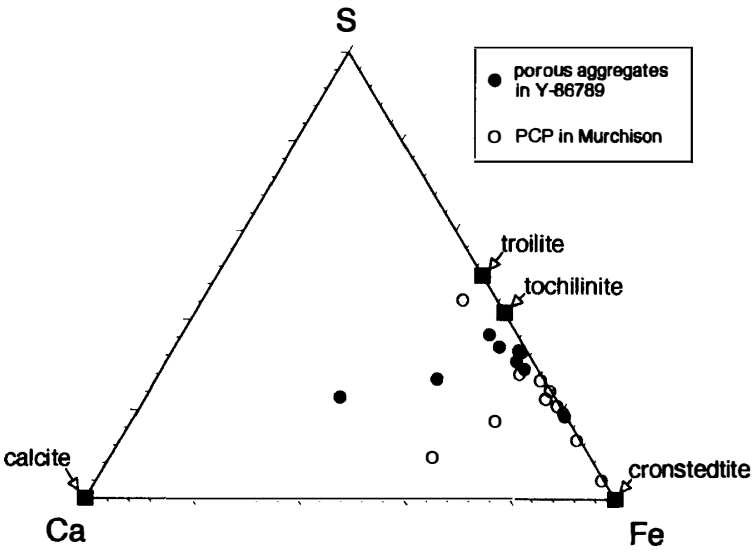

Fig. 11. Bulk compositions of the porous aggregates in the matrix and the PCP particles in the Murchison CM chondrite obtained by defocused beam analyses. Solid and open circles correspond to the compositions of the porous aggregates and the PCP particles, respectively. Solid squares show compositions of minerals in PCP. Compositional data of tochilinite is taken from BARBER *et al. (1983). This diagram shows that the porous aggregates and the PCP particles have similar compositions.*

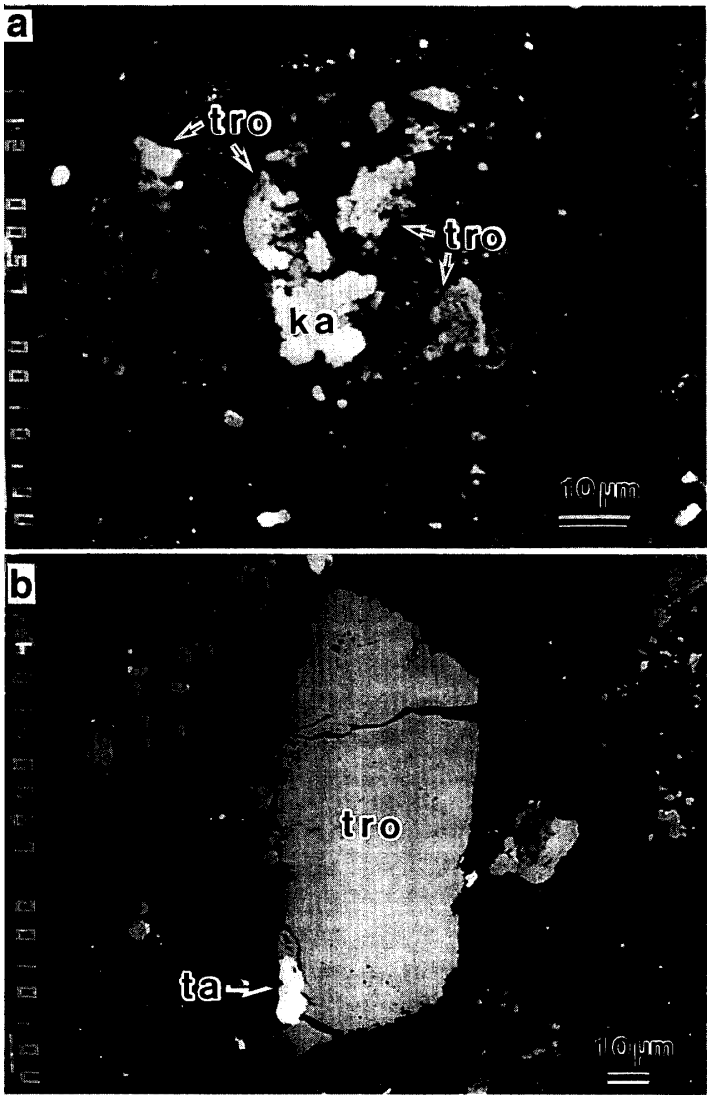

Fig. 12. A BSE image of (a) irregular-shaped troilite (tro, indicated by arrows) and kamacite (ka, a slightly bright grain) grains in a porous aggregate and (b) a troilite (tro) lath containing taenite (ta, a bright grain indicated by an arrow).

Table 5. Representative chemical compositions of sulfide and metal in Y-86789 (at%).

	Troilite			Kamacite			Taenite		
Fe	49.54	50.18	50.15	96.25	98.83	94.70	77.42	72.57	60.48
Ni	n.d.	n.d.	n.d.	1.46	0.69	4.90	22.16	27.26	39.07
S	49.78	49.49	49.56	0.15	n.d.	n.d.	n.d.	n.d.	0.15
Cr	n.d.	n.d.	n.d.	n.d.	n.d.	0.16	n.d.	n.d.	0.11
Total	99.32	99.67	99.71	97.86	99.52	99.76	99.58	99.83	99.81

n.d.: not detected

show mainly rounded or subrounded morphology (Figs. 9 and 10). The aggregates typically range from 10 to 50 μm in size and consist of small particles of troilite, kamacite and Ca-rich minerals. Bulk compositions of these aggregates are rich in Fe, S, and Ca (Table 4) and are plotted in the Fe-S-Ca ternary diagram (Fig. 11). Because Y-86789 is petrologically similar to CM chondrites, these aggregates can be interpreted as dehydrated and decomposed PCP. Figure 11 shows that the aggregates and PCP particles in the Murchison CM chondrite have similar compositions.

Unusually high abundance of opaque minerals, including those in the porous aggregates, is observed throughout the matrix (Fig. 9). Troilite is a dominant mineral and occurs in two different forms: aggregates of small, irregular-shaped grains (Fig. 12a) and large euhedral laths (Fig. 12b). The irregular-shaped grains are <1 to 50 μm in size, while the euhedral laths are 100 to 300 μm in length and 30 to 50 μm in width. Fe-Ni metal also occurs in the matrix as small grains (<10 μm in diameter) closely attached to troilite grains (Figs. 12a and b). They are kamacite ($Fe_{95}Ni_5$) and taenite whose compositions range between $Fe_{78}Ni_{22}$ and $Fe_{60}Ni_{40}$ (Table 5). Like in the chondrules, matrix materials surrounding troilite grains are Fe-rich and appear bright in BSE images (Fig. 9). These Fe-rich halos are several to a few tens microns wide, and their chemical compositions are shown in Table 2 and are plotted in Fig. 8.

4. Discussion

Our results indicate that chondrules and matrix of Y-86789 consist entirely of fine-grained phyllosilicate-like materials that have chemical compositions of a mixture of serpentine and saponite. Thus Y-86789 must have experienced extensive aqueous alteration. Quantitative chemical analyses and X-ray diffraction measurements, on the other hand, suggest that the phyllosilicate-like materials both in the chondrules and the matrix are dehydrated and composed of olivine and probably amorphus Si-rich phases. Therefore, it is concluded that Y-86789 has experienced heating and dehydration after aqueous alteration.

SOUZA SANTOS and YADA (1979) studied terrestrial serpentine heated at temperatures from 600°C to 1300°C by TEM. They observed that at 650°C the nucleation of forsterite starts, at 700°C serpentine disappears while the external morphology of the serpentine fibrils is preserved, between 800°C and 900°C forsterite becomes well-crystallized and the deformation of the external morphology of the serpentine fibrils starts, and from

1000°C to 1300°C the transformation of forsterite to enstatite is promoted and the morphology of the serpentine fibrils is completely lost. AKAI (1992) also carried out heating experiments of serpentine in the Murchison CM chondrite and observed by TEM that serpentine decomposes to olivine and enstatite through a transitional structure. On the other hand, the phyllosilicate-like materials in Y-86789 are characterized by (1) presence of olivine, (2) absence of phyllosilicate minerals such as serpentine and saponite, (3) absence of enstatite, and (4) well-preserved phyllosilicate-like fibrous texture. Thus comparison of these characteristics of Y-86789 with the previous works (SOUZA SANTOS and YADA, 1979; AKAI, 1992) yields an approximate maximum temperature of 700°C that Y-86789 experienced during dehydration stage.

Table 1 shows bulk chemical composition of Y-86789 measured by defocused electron probe and those of B-7904, Y-82162, and Y-86720 for comparison (HARAMURA *et al.*, 1983; TOMEOKA *et al.*, 1989a, b). The bulk composition of Y-86789 resembles those of B-7904 and Y-86720, but is slightly different from that of Y-82162, although FeS content and measured total weight of Y-86789 are lower than other three meteorites. In spite of dehydration of Y-86789, the total of the bulk composition is low, which may be caused by abundant pores in the matrix. The pores in Y-86789 heterogeneously distribute and are particularly abundant in the porous aggregates, where troilite grains mostly occur (Fig. 9). Because the measurement of FeS content by defocused beam is sensitive to the porosity, the lower FeS content of Y-86789 relative to other three meteorites is

Table 6. The petrological and mineralogical characteristics of CI, Y-82162, Y-86720, Y-86789, B-7904 and CM, added to IKEDA (1992).

	CI	Y-82162	Y-86720	Y-86789	B-7904	CM
H_2O(wt%) of whole rock	17-23	8.01	4.6	<5(?)	2.1	3-17
Chondrules	no	no	(+)	(+)	+	+
Al_2O_3 contents	Low	Low	Low, High	Low, High	Low, High	Low, High
PCP	no	no	no	no	no	+
Accretionary dust mantles	no	no	+	+	+	+
Primary olivine	(+)	no	no	no	+	+
Secondary olivine	no	+	+	+	+	no
Opaque minerals	Pyr, Fer Mt, Pen	Pur, Mt, Awa, Pen, Ilm	Tr, Ta, Ka, Ilm	Tr, Ta, Ka, Ilm	Tr, Ta, Ka Mt, Pen, Ilm, Chm	Toc, Mt, Pyr
Euhedral FeS laths	(+)	+	+	+	no	no
Matrix phyllosilicates	Smec, Serp	dehydrated (Smec, Serp)	dehydrated (Smec, Serp)	dehydrated (Smec, Serp)	dehydrated (Smec, Serp)	Smec, Serp
Framboidal magnetite	+	+	no	no	no	no

H_2O contents of whole rock are H_2O(+), but that of Y-86789 is estimated from presumption from EPMA analyses.

Chondrules in Y-86720 and Y-86789 are completely altered to aggregates of phyllosilicates shown here as (+).

Al_2O_3 contents are alumina of phyllosilicates or phyllosilicate-like materials in chondrules (Low and high are 0–6.5 and 6.5–26 wt% respectively).

Abbreviations: Pyr (pyrrhotite), Fer (ferrihydrite), Mt (magnetite), Pen (pentlandite), Awa (awaruite), Tr (troilite), Ta (taenite), Ka (kamacite), Ilm(ilmenite), Toc (tochilinite), Smec (smectite) and Serp (serpentine).

likely a result of an existence of troilite in the porous aggregates.

As shown in Table 6, petrographical, mineralogical and compositional characteristics of Y-86789 are similar to Y-86720: (1) absence of primary olivine which was hydrated by aqueous alteration, (2) complete replacement of chondrules by phyllosilicate minerals, (3) presence of accretionary dust mantles around chondrules, (4) abundant of secondary olivine produced by heating, (5) species of opaque minerals in the chondrules and the matrix, (6) existence of Ca-carbonate and HA-phases in some chondrules, and euhedral troilite laths in the matrix. Bulk chemical composition of Y-86789 is also similar to that of Y-86720. The matrix compositions of Y-86789 are almost identical to that of Y-86720 as reported by TOMEOKA *et al.* (1989b) (Fig. 8). Based on these similarities, we propose that Y-86789 and Y-86720 are paired. However, there is a minor difference between Y-86789 and Y-86720. Ni contents of taenite in Y-86720 range from 35 to 60 wt% (TOMEOKA *et al.*, 1989b; BISCHOFF and METZLER, 1991), while those in Y-86789 range from 23 to 38 wt% as determined from analysis of six taenite grains. Further detailed analysis is need to discuss significance of this difference.

5. Conclusions

(1) Y-86789 is an unusual CM-like carbonaceous chondrite, which has experienced extensive aqueous alteration and heating at approximately 700°C in the meteorite parent body.

(2) X-ray measurements reveal that major silicate phases in chondrules and matrix of Y-86789 are olivine, suggesting that almost all pre-existed phyllosilicate minerals are transformed to olivine and probably amorphus Si-rich phases.

(3) Y-86789 bears a close resemblance with Y-86720, thus they may be paired.

Acknowledgments

The authors thank National Institute of Polar Research for loaning the sample. They also thank Prof. N. SHIMADA for allowance to use an EPMA and a Gandolfi X-ray camera, Dr. NAMIKI for proof reading, and Mr. K. SHIMADA for assistance with the EPMA analyses.

References

AKAI, J. (1988): Incompletely transformed serpentine-type phyllosilicates in the matrix of Antarctic CM chondrites. Geochim. Cosmochim. Acta, **52**,1593–1599.

AKAI, J. (1990): Mineralogical evidence of heating events in Antarctic carbonaceous chondrites, Y-86720 and Y-82162. Proc. NIPR Symp. Antarct. Meteorites, **3**, 55–68.

AKAI, J. (1992): T-T-T diagram of serpentine and saponite, and estimation of metamorphic heating degree of Antarctic carbonaceous chondrites. Proc. NIPR Symp. Antarct. Meteorites, **5**, 120–135.

AKAI, J. (1994): Void structures in olivine grains in thermally metamorphosed Antarctic carbonaceous chondrite B-7904. Proc. NIPR Symp. Antarct. Meteorites, **7**, 94–100.

BARBER, D. J., BOURDILLON, A. and FREEMAN, L. A. (1983): Fe-Ni-S-O layer phase in C2M carbonaceous chondrites—A hydrous sulphide? Nature, **305**, 295–297.

BISCHOFF, A. and METZLER, K. (1991): Mineralogy and petrography of the anomalous carbonaceous chon-

drites Yamato-86720, Yamato-82162, and Belgica-7904. Proc. NIPR Symp. Antarct. Meteorites, **4**, 226–246.

BUNCH, T. E. and CHANG, S. (1980): Carbonaceous chondrites-II. Carbonaceous chondrite phyllosilicates and light element geochemistry as indicators of parent body process and surface condition. Geochim. Cosmochim. Acta, **44**, 1543–1577.

DUFRESNE, E. R. and ANDERS, E. (1962): On the chemical evolution of the carbonaceous chondrites. Geochim. Cosmochim. Acta, **26**, 1085–1114.

FREDRIKSSON, K. and KERRIDGE, J. F. (1988): Carbonates and sulfates in CI chondrites: Formation by aqueous activity on the parent body. Meteoritics, **23**, 35–44.

HARAMURA, H., KUSHIRO, I. and YANAI, K. (1983): Chemical compositions of Antarctic meteorites I. Mem. Natl Inst. Polar Res., Spec. Issue, **30**, 109–121.

IKEDA, Y. (1991): Petrology and mineralogy of the Yamato-82162 chondrite (CI). Proc. NIPR Symp. Meteorites, **4**, 187–225.

IKEDA, Y. (1992): An overview of the research consortium, "Antarctic carbonaceous chondrites with CI affinities, Yamato-86720, Yamato-82162, and Belgica-7904". Proc. NIPR Symp. Antarct. Meteorites, 5, 49–73.

IKEDA, Y., NOGUCHI, T. and KIMURA, M. (1992): Petrology and mineralogy of the Yamato-86720 carbonaceous chondrite. Proc. NIPR Symp. Antarct. Meteorites, **5**, 136–154.

KALLEMEYN, G. W., (1988): Compositional study of carbonaceous chondrites with CI-CM affinities. Papers Presented to the 13th Symposium on Antarctic Meteorites, June 7–9, 1988. Tokyo, Natl Inst. Polar Res., 132–134.

KIMURA, M. and IKEDA, Y. (1992): Mineralogy and petrology of an unusual Belgica-7904 carbonaceous chondrite: Genetic relationships among the components. Proc. NIPR Symp. Antarct. Meteorites, **5**, 74–119.

MAYEDA, T. K. and CLAYTON, R. N. (1990): Oxygen isotopic components of B-7904, Y-82162, and Y-86720. Papers Presented to the 15th Symposium on Antarctic Meteorites, May 30-June 1, 1991. Tokyo, Natl Inst. Polar Res., 196–197.

MCSWEEN, H. Y., Jr. (1979): Alteration in CM carbonaceous chondrites inferred from modal and chemical variations in matrix. Geochim. Cosmochim. Acta, **43**, 1761–1770.

MCSWEEN, H. Y., Jr. (1987): Aqueous alteration in carbonaceous chondrites; Mass balance constraints on matrix mineralogy. Geochim. Cosmochim. Acta, **51**, 2469–2477.

METZLER, K. and BISCHOFF, A. (1987): Accretionary dark rims in CM-chondrites. Meteoritics, **22**, 458–459.

METZLER, K. and BISCHOFF, A. (1989): Accretionary dark mantles in CM-chondrites as indicators for processes prior to parent body formation. Lunar and Planetary Science XX. Houston, Lunar Planet. Inst., 689–690.

METZLER, K. and BISCHOFF, A. (1990): Petrography and chemistry of accretionary dust mantles in the CM-chondrites Y-791198, Y-793321, Y-74662 and ALHA83100—Indications for nebula processes. Papers Presented to the 15th Symposium on Antarctic Meteorites, May 30–June 1, 1991. Tokyo, Natl Inst. Polar Res., 198–200.

METZLER, K. and BISCHOFF, A. and STÖFFLER, D. (1988): Characteristics of accretionary dark rims in carbo naceous chondrites. Lunar and Planetary Science XIX. Houston, Lunar Planet. Inst., 772–773.

METZLER, K. and BISCHOFF, A. and STÖFFLER, D. (1992): Accretionary dust mantles in CM chondrites: Evidence for solar nebula processes. Geochim. Cosmochim. Acta, **56**, 2873–2897.

RICHARDSON, S. M. (1978): Vein formation in the C1 carbonaceous chondrites. Meteoritics, **13**, 141–159.

SOUZA SANTOS, H. and YADA, K. (1979): Thermal transformation of chrysotile studied by high resolution electron microscopy. Clays Clay Miner., **27**, 161–174.

TOMEOKA, K. (1990a): Phyllosilicate veins in a CI meteorite: Evidence for aqueous alteration on the parent body. Nature, **345**, 138–140.

TOMEOKA, K. (1990b): Mineralogy and petrology of Belgica-7904: A new kind of carbonaceous chondrite from Antarctica. Proc. NIPR Symp. Antarct. Meteorites, **3**, 40–54.

TOMEOKA, K. and BUSECK, P. R. (1985): Matrix mineralogy of the Orguil CI carbonaceous chondrites. Geochim. Cosmochim. Acta, **52**, 1627–1640.

TOMEOKA, K., KOJIMA, H. and YANAI, K. (1989a): Yamato-82162: A new kind of CI carbonaceous chondrite

found in Antarctica. Proc. NIPR Symp. Antarct. Meteorites, **2**, 36–54.

TOMEOKA, K. and KOJIMA, H. and YANAI, K. (1989b): Y-86720: A CM carbonaceous chondrite having experienced extensive aqueous alteration and thermal metamorphism. Proc. NIPR Symp. Antarct. Meteorites, **2**, 55–74.

YANAI, K. and KOJIMA, H. (1987): Photographic Catalog of the Antarctic Meteorites. Tokyo, Natl Inst. Polar Res., 298p.

(Received October 11, 1995; Revised manuscript accepted January 10, 1996)